

Measuring the 'Great Unconformity' on the North China Craton using new detrital zircon age data

Tianchen He^{1*}, Ying Zhou¹, Pieter Vermeesch¹, Martin Rittner¹, Lanyun Miao², Maoyan Zhu², Andrew Carter³, Philip A. E. Pogge von Strandmann^{1,3} & Graham A. Shields¹

¹ *Department of Earth Sciences, University College London, Gower Street, London WC1E 6BT, UK*

² *State Key Laboratory of Palaeobiology and Stratigraphy, Nanjing Institute of Geology and Palaeontology, Chinese Academy of Sciences, Nanjing 210008, China*

³ *Department of Earth and Planetary Sciences, Birkbeck College, University of London, Malet Street, London WC1E 7HX, UK*

*Corresponding author (e-mail: tianchen.he.13@ucl.ac.uk)

Abstract: New detrital zircon ages confirm that Neoproterozoic strata of the southeastern North China Craton (NCC) are mostly of early Tonian age, but that the Gouhou Formation, previously assigned to the Tonian, is Cambrian in age. A discordant hiatus of >150-300 million years occurs across the NCC, spanning most of the late Tonian, Cryogenian, Ediacaran and early Cambrian periods. This widespread unconformable surface is akin to the 'Great Unconformity' seen elsewhere in the world, and highlights a major shift in depositional style from largely erosional, marked by low rates of net deposition, during the mid-late Neoproterozoic to high rates of transgressive deposition during the mid-late Cambrian. Comparison between age spectra for southeastern NCC and northern India are consistent with a provenance affinity linking the NCC and East Gondwana by ~510 Ma.

Supplementary material: The full sample list and U-Pb data are available at:

It has long been recognized that the traditional Precambrian–Cambrian (Ediacaran–Cambrian) boundary interval is characterized worldwide by low rates of deposition and/or a major unconformity, known as the 'Great Unconformity' (Brasier & Lindsay 2001, Peters & Gaines 2012). Global eustatic sea-level rise and widespread orogenesis accompanied the Cambrian bioradiation, and have both been linked to unprecedented high flux rates for nutrients and other dissolved ions during the late Neoproterozoic and early Paleozoic (Meert & Lieberman 2008, Squire *et al.* 2006, Campbell & Allen 2008). Enhanced chemical weathering on the 'Great Unconformity' during transgression has been causally linked to the Cambrian explosion (Peters & Gaines 2012), in particular the introduction of skeletal biomineralisation. In support of this, Brasier and Lindsay (2001) identified a number of regions

of the world where deposition rates increased remarkably after the Ediacaran–Cambrian boundary, in a transgressive episode marked by widespread phosphogenesis. One such area is the southeastern North China Craton (NCC), which possesses well-exposed Neoproterozoic–Cambrian marine successions with astonishingly well-preserved, organic-walled fossils (Zang & Walter 1992, Dong *et al.* 2008, Xiao *et al.* 2014, Tang *et al.* 2015). However, the full potential of these exceptional paleontological archives cannot be realized until uncertainties in the depositional ages and stratigraphic correlations across the NCC are resolved (Xiao *et al.* 2014).

The 'Great Unconformity' is unambiguously recognised in large parts of the world where this contact is represented by a nonconformity. However, it is much more challenging to identify this contact in other regions, including the Canadian Rocky Mountains (Aitken 1969), South Australia (Nedin *et al.* 1991) and the NCC, where this surface is commonly preserved as a cryptic disconformity, separating thick successions of Neoproterozoic strata from overlying Cambrian ones. Uncertainty remains surrounding the stratigraphic level of the lowermost Cambrian as well as the positioning of the major break that is regionally traceable along the southeastern margin of the NCC. Precise age constraints on individual formations are needed to locate the position of this significant gap in successions that potentially may exhibit a number of disconformable levels (Wang *et al.* 1984, Hong *et al.* 1991) and to resolve the timing and duration of the coeval uplift events and/or sea-level fluctuations. In addition, recent palaeogeographic reconstructions, e.g. in which the NCC was attached to East Gondwana (McKenzie *et al.* 2011b, Han *et al.* 2016) or was an isolated continent (Zheng-Xiang Li *et al.* 2013, Cocks & Torsvik 2013, Torsvik & Cocks 2013, Wilhem *et al.* 2012) during the Cambrian, are not yet fully grounded. Detrital zircon analysis can be used to address these uncertainties to 1) establish the maximum depositional age of sedimentary units; 2) identify the missing age interval such as depositional breaks in stratigraphic successions in the absence of a robust biostratigraphic framework; 3) use provenance comparison of age modes to build up interbasinal stratigraphic correlations and 4) reconstruct the fragmentation and affinity history of different continental plates of the geological past (Fedo 2003).

This paper presents new detrital zircon U-Pb age data for 13 Neoproterozoic–Cambrian samples from the Huaibei and Dalian regions, which are situated along the southeastern margin of the NCC. Combining our new age constraints with published radiometric ages of detrital zircons and intrusive diabase sills, we provide refined age constraints on stratigraphic successions and attempt to resolve the major depositional breaks in Neoproterozoic–Cambrian successions of the southeastern NCC. The

provenance of age components identified in these samples is also interpreted with respect to regional stratigraphic correlation and palaeogeographic reconstruction.

Regional stratigraphic context and sample localities

The Huaibei and Dalian regions are geologically situated at the southeastern margin of the NCC, and are located along the rims of the Jiao-Liao-Ji belt (Fig. 1), which is a Paleoproterozoic orogenic belt (~1.9 Ga) that divides the eastern Block of the NCC into two sub-blocks in the northwest (Longgang Block) and southeast (Langrim Block) (Zhao *et al.* 2005). Neoproterozoic–Cambrian successions are well exposed, including the Huaibei Group in Huaibei region and Jinxian Group in Dalian region. Given that both regions were contiguous during the Neoproterozoic–Cambrian transition, they share a similar litho- and biostratigraphic record (Wang *et al.* 1984, Hong *et al.* 1991, Xiao *et al.* 2014). However, neither of these formal lithostratigraphic groups follow international standard practice in that their included formations, although contiguous, do not have ‘significant and diagnostic lithologic properties in common’ (Murphy & Salvador 1999). In both regions, one could easily argue that the topmost formation has more in common with overlying Cambrian units, which are characterised by a reddish colour, evaporite pseudomorphs and planar-bedded mottle limestone, than with those beneath, which are characterised by stromatolitic build-ups and molar-tooth structure. In this study, we focus on the upper parts of the Huaibei and Jinxian groups and their adjacent Cambrian strata (Fig. 2).

Huaibei region

In general, the upper part of the Huaibei Group constitutes a sequence of carbonate and siliciclastic deposits, including the Shijia, Wangshan, Jinshanzhai and Gouhou formations in ascending stratigraphic order (Fig. 2). The Shijia Formation was sampled at the Heifengling section (Fig. 1), and is characterized by pale yellowish green and reddish purple shale with interbeds of quartz sandstone and stromatolitic dolostone. The succeeding Wangshan, Jinshanzhai and Gouhou formations were investigated at Gouhou and Jinshanzhai sections (Fig. 1). The Wangshan Formation is dominated by dolomitic or cherty limestone with the presence of abundant ‘molar tooth’ structures and stromatolite forms, including *Acaciella*, *Anabaria*, *Inzeria* that would be consistent with a pre-Cryogenian age (Qian *et al.* 2002). The Jinshanzhai Formation consists of green and reddish purple shale interbedded with glauconitic quartz sandstone in the lower part, while the upper part is characterized by purple stromatolitic dolostone with stromatolite forms, including *Boxonia*, *Linella* and *Xiejiella* (Qian *et al.* 2002). The Gouhou Formation, which is the uppermost unit of the Huaibei Group, is subdivided into two parts in this study. The lower ‘member’ is dominated by red clastic rocks, while the upper

'member' consists of pale grey, cherty dolostone (Fig. 3e, 3g & 3h). Halite pseudomorphs are present in both clastic (Fig. 3f) and carbonate intervals, which together with abundant mud cracks in the lower member indicate an evaporitic, likely marginal marine environment was maintained throughout deposition of the Gouhou Formation. Algal fossils are reported from the Jinshanzhai and Gouhou formations in the form of carbonaceous compressions of the genera *Protoarenicola* (Jinshanzhai Fm.) and *Chuaria*, *Ellipsophysa* and *Tawuia* (Gouhou Fm.), respectively (Zang & Walter 1992, Dong *et al.* 2008).

The lower contacts of the Jinshanzhai and Gouhou formations have both been suggested to coincide with the Precambrian–Cambrian boundary in the Huaibei region (Qian *et al.* 2001). However, these two formations are now thought to have been deposited during the Tonian Period based on the co-occurrence of a possible 'Tonian-age' acritarch organic-walled microfossil assemblage that includes *Trachyhystrichosphaera*, *Valeria*, and *Dictyosphaera* at a single level within the lower Gouhou Formation (Tang *et al.* 2015). Although this Tonian assignment is consistent with reports of a *Chuaria*-*Tawuia* association in the same formation (Xiao *et al.* 2014, Tang *et al.* 2015), the validity of acritarch biostratigraphy for age determination in the Precambrian is less well established than for the Phanerozoic, and may have limitations due to relatively poor species classification and long-range distribution in the geological record. Moreover, as shown in Fig. 3g & 3h, some beds within the upper Gouhou Formation, in which halite pseudomorphs are conspicuously absent, are characterised by mottled fabrics that we compare with the pervasive bioturbation that is characteristic of the Phanerozoic, although no nameable ichnofossils have yet been identified. Given that the oldest ichnofabrics are no older than late Ediacaran in age (Rogov *et al.* 2012), it seems reasonable to question the assigned Tonian affinity of the Gouhou Formation. The unambiguously Cambrian Houjiashan and Mantou formations overlie the Huaibei Group with apparent conformity at Gouhou and Jinshanzhai sections. The Houjiashan Formation consists of yellowish dolomitic shale at the base, followed by extensively bioturbated thick-bedded, intrasparitic limestone. The trilobites *Estiaingia* and *Redlichia* characterize the Houjiashan Formation, indicative of the Canglangpuan Stage = lower part of Cambrian Stage 4, (~515 Ma) (Zhang & Zhu 1979, Miao 2014). The Mantou Formation overlies the Houjiashan Formation, and its lower part is characterized by red shale and *Redlichia*, consistent with the Longwangmiaoan Stage = upper part of Cambrian Stage 4 (~510 Ma).

Dalian region

The upper part of the Jinxian Group consists of the Xingmincun, Getun and Dalinzi formations in ascending stratigraphic order (Fig. 2). The Xingmincun Formation comprises glauconite-bearing clastic

rocks in the lower to middle parts, and dark grey thin-medium bedded limestone in the upper part (Fig. 4a & 4b). Discoid fossils of probable pre-Ediacaran age are reported in shale of the middle part of the formation (Hong *et al.* 1991, Luo *et al.* 2016), while recently published radiometric ages confirm that the Xingmincun Formation was deposited in the Tonian Period (Yang *et al.* 2012, Zhang *et al.* 2016). The Getun and Dalinzi formations were sampled at Manjiatan and Longwangmiao sections (Fig. 1). The Getun Formation is dominated by clastic rocks (Fig. 4c, 4d & 4e) with some stromatolitic horizons and the carbonaceous compression fossils *Chuaria* and *Tawuia* (Hong *et al.* 1991). *Archaeostracods* (bradoriids) were reported from the upper part of the Getun Formation, implying a Qiongzhusinian or Cambrian Age 3 affinity (~520-515 Ma) (Wang & Yang 1986) but these findings have not been confirmed. The Dalinzi Formation consists of yellowish green and reddish purple sandstone (Fig. 4f) with thin-bedded light grey dolostone in the topmost beds (Fig. 4h). The small shelly fossil *Sachites* of Cambrian Fortunian Age-Age 3 affinity was reported from the red shale of the upper Dalinzi Formation (Hong *et al.* 1991). Mud cracks, halite casts (Fig. 4g), thin-layered gypsum deposits and cross-bedding are all observed in both the Getun and Dalinzi formations, suggesting that the units were probably formed in a shallow marine evaporitic environment. Indeed, the Getun and Dalinzi facies have been interpreted to represent a lagoonal and playa lake or other evaporative setting, respectively (Fairchild *et al.*, 2000). Also noteworthy is the observation that these features are also found in the Gouhou Formation (Huaibei region), which is dominated in its lower-middle part by clastic rocks, which are gradually replaced by dolostone in the upper part, possibly due to a widespread marine transgression that resumes through the overlying formations. The Cambrian Jianchang and Mantou formations overlie the Jinxian Group. The Jianchang Formation is dominated by dark grey medium-thick bedded limestone. Co-occurrence of the *Latipalaeolenus* trilobite assemblage (Hong *et al.* 1991, Liu 2012) and archaeocyath assemblages (Hong *et al.* 1990) indicates that the unit can be approximately correlated with the Houjiashan Formation in the Huaibei region (Fig. 6). The overlying Mantou Formation is characterized by red shale and *Redlichia*, and so is consistent with the Mantou Formation in the Huaibei region.

Importantly, many hypotheses regarding the placement of the Neoproterozoic–Cambrian boundary in the region appear to be debatable. Some propose the Getun Formation (also referred to as ‘Gejiatun Formation’) as the lowermost Cambrian unit (Wang & Yang 1986, Duan & An 1994, Qiao 2002), while others favour a boundary at the top of the Dalinzi Formation (Hong *et al.* 1991, Xue *et al.* 2001). However, these arguments are largely based on the unsubstantiated occurrence of Cambrian ichnofossils and small shelly fossils, highlighting the importance of precise and accurate radiometric dating of these formations.

Unconformable stratigraphic contacts

Various observations have been made regarding the possible location of the major unconformity among multiple candidates between Neoproterozoic and Cambrian strata on the southeastern NCC. In the Huaibei region, the Jinshanzhai Formation sits with clear erosional unconformity on top of the Wangshan Formation, evidenced at its base by a widespread conglomeratic bed that marks an abrupt lithological change from carbonate to siliciclastic rocks (Fig. 3a & 3b). Another abrupt change in lithology and a conglomerate bed can be observed between the Gouhou and Jinshanzhai formations (Fig. 3c), indicating the existence of a second possible depositional gap, although the clasts in this case are smaller, more angular and potentially derived from underlying strata at the Jinshanzhai section (Fig. 3d). Regional mapping reveals that the Houjiashan Formation overlies various Neoproterozoic formations, which are reddened at their tops, identifying its base as a major transgressive surface (Li *et al.* 2013, Xiao *et al.* 2014), but without clear indication of an erosional unconformity. At sections where the Houjiashan Formation overlies the Gouhou Formation, there is no reddening or other sign of surface exposure at the top of the Gouhou Formation. However, the top of the Jinshanzhai Formation comprises reddened stromatolites, which directly underlie the red beds of the lower Gouhou Formation.

In the Dalian region, potentially significant erosional disconformities are reported overlying the Xingmincun (Fig. 4a), Getun and Dalinzi formations (Fig. 4h), respectively (Hong *et al.* 1991). By contrast, others have observed no major lithological or facies changes between the Getun and Dalinzi formations, implying a conformable contact (Wang & Yang 1986, Duan & An 1994, Qiao 2002). The Getun/Xingmincun boundary is marked in the field by the abrupt appearance of black shale overlying a basal lag conglomerate (Fairchild *et al.* 1997, Fairchild *et al.* 2000), which lies directly on top of bluish dolomitic limestone of the upper Xingmincun Formation (Fig. 4a & 4b). The Getun Formation is not always well exposed in the Dalian region and is interrupted by diorite sills at Manjiatan section, where there are potentially significant erosional surfaces within it (Fig. 4c). A transitional contact is suggested between the fine-grained, shaly upper Getun and sandy lower Dalinzi formations (Fig. 4d). However, black chert lonestones are exposed near the contact (Fig. 4e), indicating another possible erosional surface. Despite equivocal support for major disconformable surfaces from sedimentary evidence, the timing and duration of these proposed hiatus surfaces remain unresolved due to a lack of a reliable chronostratigraphic framework and to some extent the lack of regional continuity of outcrop due in part to recent urban development and widespread igneous intrusions of Neoproterozoic–Mesozoic age.

Materials and methods

13 samples of clastic rock from the Shijia, Jinshanzhai, Gouhou, Getun and Dalinzi formations were taken at different stratigraphic intervals within the individual formations. Poorly sorted and coarser samples were selected in the field as they likely represent better mixed detrital sources, and zircons of larger grain size are preferred for laser ablation and dating precision. Sample lithologies, GPS locations and a compiled U-Pb age dataset are reported in the supplementary information. Zircon grains were separated using standard mineral separation procedures, which include jaw crushing, sieving, magnetic and heavy liquids separation. Handpicked zircons were then mounted in epoxy and polished prior to analysis. In-situ zircon U-Pb dating was carried out at the London Geochronology Centre, University College London, using a New Wave 193 nm excimer laser ablation system, coupled to an Agilent 7700x quadrupole ICP-MS. Real time data were processed using GLITTER 4.4 data reduction software. Repeat measurements of external zircon standard Plešovice (TIMS reference age 337.13 ± 0.37 Ma) (Sláma *et al.* 2008) and NIST 612 silicate glass (Pearce *et al.* 1997) were used to correct for instrumental mass bias and depth-dependent inter-element fractionation of Pb, Th and U. Around 150 grains were analyzed for each sample in order to meet established requirements for provenance studies as suggested in Vermeesch (2004). Normalized age kernel density estimate plots (Fig. 5) were produced utilizing software package ‘*provenance*’ (Vermeesch *et al.* 2016). Maximum deposition ages in Fig. 5 are calculated by the youngest cluster in the detrital zircon U-Pb age spectra using the minimum age model of Galbraith (2005) as implemented in the ‘*DensityPlotter*’ software (Vermeesch 2012).

U-Pb data

Detrital zircon U-Pb results from Dalian and Huaibei regions are presented separately as Kernel density estimate plots (Fig. 5). In Huaibei Group, the Shijia Formation zircons exhibit a broad range of ages between 0.9 Ga and 2.0 Ga, with the main peak at ca. 1.2 Ga. The Jinshanzhai Formation yielded no grains younger than 0.8 Ga, with an age distribution dominated by a large population with peak centering at ca. 2.1 Ga. The overlying Gouhou Formation exhibits a broad population of zircons, with an isolated age population of around 0.5 Ga, two prominent peaks at approximately 1.85 Ga and 2.5 Ga as well as a smaller population of Neoproterozoic to Mesoproterozoic age. The Cambrian-age group comprises 8 concordant zircon grains from three samples that were collected at different stratigraphic horizons within the Lower Gouhou Formation from two separate sections (see supplementary information). Ages of these grains range from 490.4 ± 5.9 Ma to 519.2 ± 5.9 Ma. Utilizing the minimum age algorithm with normal errors (Galbraith 2005), a statistical estimate age of

518.4±2.9 Ma for the youngest age mode is suggested here to represent the maximum depositional age for the Gouhou Formation. Previously reported age spectra for the Jinshanzhai Formation shows peaks centered at 1.85 Ga and 2.5 Ga (Yang *et al.* 2012), similar to the patterns from our Gouhou Formation samples. However, both samples of the Jinshanzhai Formation in our study show distinctive 2.1 Ga peaks, which are strikingly absent in the published study.

For the Jinxian Group, the Xingmincun Formation yielded prominent populations of around 0.9-1.1 Ga and 1.5-1.8 Ga (Yang *et al.* 2012). The overlying Getun Formation yielded a considerable number of grains between 0.7 Ga and 1.0 Ga. As with the Gouhou Formation, the Dalinzi Formation contains one prominent peak at 1.85 Ga and two smaller peaks at ca. 0.7 Ga and 2.5 Ga. The lowermost Cambrian Myeonsan Formation from eastern Korea yielded similar age spectra to Gouhou and Dalinzi formations with dominant peaks at 1.85 Ga and 2.5 Ga (Lee *et al.* 2016, Cho & Cheong 2016, Kim & Ree 2016).

Depositional age constraints

New and compiled detrital zircon U-Pb age populations in Fig. 5 likely reflect the ages of dominant magmatism in the southeastern NCC. Maximum depositional ages of each formation are determined by the ages of the youngest group of detrital zircons. In addition, minimum depositional ages are constrained by U-Pb baddeleyite or zircon crystallization ages of cross-cutting diabase sills (Fig. 2). In the Huaibei region, detrital zircon data show that the Shijia and Wangshan formations were most likely deposited between 950 Ma and 820 Ma; zircon data from sills and likely correlation with correlative strata in the Dalian region indicate a depositional age most probably closer to the older end of that age range (Zhang *et al.* 2016). There is no general agreement regarding the depositional age of the Jinshanzhai and Gouhou formations of the uppermost Huaibei Group, with diverse interpretations from Cambrian (Xing 1996, Zang & Walter 1992), Cryogenian–Ediacaran (Cao 2000, Wang *et al.* 1984) to Tonian ages (Xiao *et al.* 2014). However, given that the youngest zircon grains yield a maximum depositional age of 518 Ma (Fig. 5), the Gouhou Formation, consistent with evidence for possible bioturbation (Fig. 3g & 3h), appears to be of similar mid-Cambrian age to the overlying trilobite-bearing Houjiashan Formation. This conclusion would appear to contradict the evidence from the acritarchs, including *Trachyhystrichosphaera aimika* and *Valeria lophostriata*, that would indicate a Tonian age (Tang *et al.* 2015). Possible explanations for this include an unexpectedly long-range distribution for several typically Tonian acritarchs and reworking of fossil fragments from older sediments. Neither of these possibilities seems perfectly satisfactory as the reported Tonian assemblage is both diverse and apparently well preserved. These results also argue against correlating

the negative $\delta^{13}\text{C}_{\text{carb}}$ excursion in the Gouhou Formation with the Tonian Bitter Springs anomaly in South Australia (Xiao *et al.* 2014) as this interval, ~ 0.8 Ga, would seem to be entirely missing on the North China Craton. Although the Jinshanzhai Formation can only be constrained with a maximum depositional age of ca. 820 Ma (Fig. 5), we consider that the Jinshanzhai Formation was deposited significantly before the Gouhou Formation, due to its entirely different character, with as much as 300 million years between them.

In the Dalian region, the depositional age of the Xingmuncun Formation is approximately constrained as between 924 Ma and 886 Ma (Yang *et al.* 2012, Zhang *et al.* 2016), and is thus confirmed as Tonian in age, which refutes the official interpretation, which assigns the entire Jinxian Group, including the Xingmuncun Formation, to the Ediacaran System (National Commission on Stratigraphy of China & China Geological Survey 2014). On the other hand, these data indicate that the overlying Getun and Dalinzi formations of the uppermost Jinxian Group formed much later than the Tonian with maximum depositional ages of 733 Ma and 711 Ma, respectively. Importantly, this compiled age framework confirms that most of the Neoproterozoic strata in southeastern NCC were deposited no later than the early Tonian Period (Xiao *et al.* 2014), and thus are considerably older than the Neoproterozoic successions of South China (Shields-Zhou *et al.* 2012, Xiao *et al.* 2012), with which they have traditionally been compared (Zang and Walter, 1992). Cryogenian–Ediacaran age strata that might be correlative with the South China successions may be absent, but if present could conceivably be represented by the highly localised, glaciogenic Fengtai and Luoquan formations of Anhui and Henan provinces, respectively (Fig. 6).

Where is the major hiatus between the Neoproterozoic and Cambrian on the NCC?

A major hiatus was proposed above the Gouhou Formation in the Huaibei region, implying a time gap spanning almost 300 million years between the Tonian (~ 0.8 Ga) to the Cambrian (~ 0.5 Ga) interval (Xiao *et al.* 2014, Tang *et al.* 2015). However, new age constraints here reveal that the Gouhou Formation and the overlying Houjiashan Formation are both Cambrian in age, with a more likely major depositional gap being placed between the Jinshanzhai and Gouhou formations, but involving an equivalently large depositional hiatus of up to 300 million years. A minor disconformity may still exist between the Gouhou and Houjiashan formations – the transition between them is commonly poorly exposed in the region – but based on the data presented here it is unlikely to be significant.

In the Dalian region, utilizing the minimum depositional age of the Xingmuncun Formation and the maximum age of the Getun Formation, the hiatus in between can be constrained to a minimum time

gap of roughly 150 million years. In this regard, it should be noted that much of the Tonian–Cambrian interval witnessed global-scale glaciations (Fig. 6), while the North China craton was subject to regional glaciation possibly during the Ediacaran Period, all of which makes it seem unlikely that the Getun and Dalinzi formations were deposited earlier than 635 Ma. This would make the hiatus at least as long as ~250 million years, and possibly much longer. Although some suggest that the Getun and Dalinzi formations are in conformable contact (Wang & Yang 1986, Duan & An 1994, Qiao 2002), it is still plausible that a second hiatus could be situated between them as suggested by the clast-enriched horizon near the Dalinzi/Getun boundary (Fig. 4e) and other studies (Hong *et al.* 1991, Xiao *et al.* 2014, Luo *et al.* 2016). A more satisfactory resolution of their depositional ages awaits more convincing fossil evidence and improved age constraints. Notwithstanding the lack of detrital zircon grains younger than ~0.7 Ga in the Getun and Dalinzi formations, putative age-diagnostic fossils could place their ages as young as early Cambrian (Wang & Yang 1986, Hong *et al.* 1991). Thus, both formations could still represent transgressive lower Cambrian strata overlying a great hiatus, thus allowing approximate temporal correlation with the lithologically similar Gouhou Formation of the Huaibei region. As argued above, the Dalinzi and Gouhou formations are significantly different in a lithological sense from underlying formations of the same group which raises question about the traditional definitions of the Huaibei and Jinxian groups.

It is noteworthy that the age spectra of the Dalinzi and Gouhou formations are similar to each other, with peaks at ca. 1.85 Ga and 2.5 Ga, and are thus distinct from other formations of the Huaibei and Jinxian groups (Fig. 5). The apparent change in detrital zircon sources coincides with the regionally expressed unconformity outlined above, reflecting perhaps a major tectonic uplift event, which affected the southeastern margin of the NCC during the Neoproterozoic–Cambrian transition. Furthermore, as illustrated in Fig. 6, this unconformable surface is ubiquitously developed over the NCC and adjacent eastern Korea terrain. It is always underlain by Precambrian rocks and overlain by Cambrian-age strata that yield trilobite (Zhang & Zhu 1979, Liu 2012, Miao 2014), archaeocyathid (Hong *et al.* 1990) and small shelly fossils (Pei & Feng 2005) of approximate Cambrian Age 4 (~515–510 Ma) affinity. The widespread erosion surface developed across southeastern NCC is considered equivalent to the globally recognized ‘Great Unconformity’ that separates Cambrian-aged sediments (~510 Ma) from underlying Precambrian units elsewhere in the world (Brasier & Lindsay 2001, Peters & Gaines 2012).

Detrital zircon provenance and palaeogeographic implications

All samples of NCC share a common age-population around 0.9-1.0 Ga. Grains of this age in the Tonian clastic units could be sourced from the early Neoproterozoic large igneous province (LIP), which is evidenced by the widespread mafic sills and dykes (0.92-0.85 Ga) in southeastern NCC (Wang *et al.* 2012, Zhang *et al.* 2016, Zhai *et al.* 2015). However, mafic magmatism is generally not associated with zircon mineralisation. The Jinshanzhai and Xingmuncun formations yielded additional, distinct peaks at approximately 2.1 Ga and 1.7 Ga, respectively. These ages probably include the reworking of mineral grains formed during the early Paleoproterozoic rifting magmatism (2.2-1.9 Ga) on the eastern continental margin of the NCC (Zhao *et al.* 2005) and the ~1.72 to 1.62 Ga anorogenic magmatic association that affected the NCC (Zhai *et al.* 2015).

Distinctively, the Cambrian Dalinzi and Gouhou formations exhibit prominent zircon clusters of 1.8-1.9 Ga and 2.5 Ga that are absent in their respective underlying formations. Voluminous granitoids, TTG gneiss and mafic volcanic rocks with ages of about 2.5 Ga are known to be widespread and account for 90% of the total exposure of Archean basement on the NCC (Zhao 2013), while the 1.8-1.9 Ga events are consistent with the assemblage of Longgang and Langrim blocks to form Jiao-Liao-Ji belt as well as the collision of the eastern and western Blocks that resulted in the final amalgamation of the NCC at ca. 1.85 Ga (Zhao *et al.* 2005, Yang *et al.* 2012, Zhao 2013).

Zircons of ~0.7 Ga age are only recovered in strata (including Getun, Dalinzi and Gouhou formations), which overlie the major hiatus in their respective regions. However, no Cryogenian igneous sources are known from the NCC, which possibly indicates that an exterior source supplied these detrital minerals. Previous studies proposed that the NCC was approaching northern India or western Australia during the Neoproterozoic–Cambrian interval (Lin *et al.* 1985, McKenzie *et al.* 2011b, Myrow *et al.* 2015), and possibly collided with northern margin of East Gondwana in the late Cambrian at ca. 500 Ma (Han *et al.* 2016). There is also strong trilobite faunal evidence, which suggests biogeographic links between NCC and East Gondwana (McKenzie *et al.* 2011b, Miao 2014). Western Australia and northern India, which occupied the northern margin of East Gondwana during the Cambrian, were apparently affected by Cryogenian magmatism during the breakup of Rodinia (Hoffman 1999, Van Lente *et al.* 2009, Hofmann *et al.* 2011, Rao *et al.* 2012). The occurrence of ca. 0.7 Ga detrital zircons on the southeastern NCC supports proximity to Gondwana much earlier than the eventual collision in the Cambrian. Additionally, zircons of 0.9-1.0 Ga age are a characteristic of source regions in East Gondwana and are found in blocks that lay adjacent to this margin of Gondwana such as South China (Cawood *et al.* 2013). This raises the possibility that East Gondwana served as an additional source of the zircon grains of early Tonian age in the Cambrian clastic units of the southeastern NCC.

Comparing with their equivalent strata in northern India (Hughes *et al.* 2010), clastic rocks of Cambrian Age 4-5 from southern NCC (McKenzie *et al.* 2011b) and eastern Korea (Lee *et al.* 2016) show strong similarity in age spectra with a dominant age population of 0.5-1.0 Ga, confirming the close affinity between NCC and East Gondwana in the Cambrian (McKenzie *et al.* 2011b). We note that these samples include those from Cambrian Stage 4-5 Mantou Formation that is stratigraphically younger than the Gouhou and Dalinzi formations of the NCC, as well as from the Myobong Formation that overlies the Myeonsan Formation in eastern Korea (Fig. 6). Gouhou, Dalinzi and Myeonsan formations, which lie directly above the regional unconformity and represent the lowermost Cambrian strata, share similar age spectra patterns with a dominant age population of 1.8-1.9 Ga (Fig. 5), but do not match the lowermost Cambrian strata from northern India, which show a widespread and distinctive population of 1.7-1.8 Ga instead (Myrow *et al.* 2010, McKenzie *et al.* 2011a, Turner *et al.* 2014). The similarities of age spectra of Cambrian stage 4-5 strata between southeastern NCC and northern India possibly imply that the East Gondwana provided detritus to the southeastern NCC in the Cambrian. On the other hand, inconsistencies at the lowermost Cambrian horizons indicate that local Archean–Paleoproterozoic basement sources appear still to have dominated the southeastern margin of the NCC at ca. 515 Ma, but these sources were replaced by shared trans-Gondwanan Neoproterozoic–Cambrian sources following the final collision of the NCC and East Gondwana, probably during the late Cambrian Age 4 to Cambrian Age 5 (Han *et al.* 2016).

Conclusions

This study provides a refined geochronological framework for the upper Huaibei and Jinxian groups overlying the southeastern North China Craton. The results confirm that the Neoproterozoic units were deposited during the early Tonian Period, while the Gouhou Formation of the uppermost Huaibei Group is shown to be Cambrian in age. A regional unconformity is revealed between the Gouhou and the Jinshanzhai formations of the Huaibei region as well as between the Getun and Xingmuncun formations of the Dalian region. This vast erosional surface can be traced across the craton and is interpreted here to be equivalent to the ‘Great Unconformity’ that marks the regional base of the Cambrian System, and neither of the Huaibei and Jinxian groups follow international standard practice in that their included formations, although contiguous, do not have ‘significant and diagnostic lithologic properties in common’ (Murphy & Salvador 1999). The magnitude of this depositional gap is constrained to be greater than 150 to 300 million years. Provenance analysis of the detrital zircon age spectra suggests that, during the Neoproterozoic–Cambrian transition, the southeastern NCC experienced exposure and weathering of the Archean–Paleoproterozoic basement, possible

denudation of a Tonian large igneous province as well as a possible contribution from Gondwana sources sometime during the Cryogenian–Cambrian interval. These data also suggest that the detrital provenance of southeastern NCC did not fully overlap with that of northern margin of East Gondwana until ca. 510 Ma.

Acknowledgements and Funding

This project was funded by the NERC research programme ‘Long-term Co-evolution of Life and the Planet’: project ‘*Re-inventing the planet: the Neoproterozoic revolution in oxygenation, biogeochemistry and biological complexity*’ (NE/1005978/1) and National Key Basic Research Program of China Grant (2013CB835004). We thank Minchen Wang and Dr Da Li for assistance in the field. Tianchen He is supported by an Overseas Research Scholarship (ORS) from University College London and a PhD scholarship from the China Scholarship Council (CSC). This article is dedicated to the memory of Martin Brasier, an inspirational teacher and renowned scholar of the Ediacaran–Cambrian boundary who accompanied TH, YZ, LM and GS to Huaibei in 2014.

References

- AITKEN, J.D. 1969. Documentation of the sub-Cambrian unconformity, Rocky Mountains Main Ranges, Alberta. *Canadian Journal of Earth Sciences*, **6**, 193–200, doi: 10.1139/e69-018.
- BRASIER, M.D. & LINDSAY, J.F. 2001. Did supercontinental amalgamation trigger the ‘Cambrian explosion’? In: Zhuravlev, A. Y. & Riding, R. (eds) *The Ecology of the Cambrian Radiation*. New York, Columbia University Press, 69–89.
- CAMPBELL, I.H. & ALLEN, C.M. 2008. Formation of supercontinents linked to increases in atmospheric oxygen. *Nature Geoscience*, **1**, 554–558, doi: 10.1038/ngeo259.
- CAO, R. 2000. Discussion on some problems in the Mesoproterozoic and Neoproterozoic stratigraphical study in China. *Journal of Stratigraphy*, **24**, 1–7.
- CAWOOD, P.A., WANG, Y., XU, Y. & ZHAO, G. 2013. Locating South China in Rodinia and Gondwana: A fragment of greater India lithosphere? *Geology*, **41**, 903–906, doi: 10.1130/G34395.1.
- CHO, M. & CHEONG, W. 2016. Comments on ‘Detrital zircon geochronology and Nd isotope geochemistry of the basal succession of the Taebaeksan Basin, South Korea: Implications for the Gondwana linkage of the Sino-Korean (North China) Block during the Neoproterozoic–early Cambrian’ by . *Palaeogeography, Palaeoclimatology, Palaeoecology*, **459**, 606–609, doi: 10.1016/j.palaeo.2016.04.024.
- COCKS, L.R.M. & TORSVIK, T.H. 2013. The dynamic evolution of the Palaeozoic geography of eastern Asia. *Earth-Science Reviews*, **117**, 40–79, doi: 10.1016/j.earscirev.2012.12.001.

441 DONG, L., XIAO, S., SHEN, B., YUAN, X., YAN, X. & PENG, Y. 2008. Restudy of the worm-like carbonaceous
 442 compression fossils Protoarenicola, Pararenicola, and Sinosabellidites from early
 443 Neoproterozoic successions in North China. *Palaeogeography, Palaeoclimatology,*
 444 *Palaeoecology*, **258**, 138–161, doi: 10.1016/j.palaeo.2007.05.019.

445 DUAN, J. & AN, S. 1994. On the subdivision and correlation for upper Precambrian System in south
 446 Liaoning Province, China. *Liaoning Geology*, **1–2**, 30–43.

447 FAIRCHILD, I.J., EINSELE, G. & SONG, T. 1997. Possible seismic origin of molar tooth structures in
 448 Neoproterozoic carbonate ramp deposits, north China. *Sedimentology*, **44**, 611–636, doi:
 449 10.1046/j.1365-3091.1997.d01-40.x.

450 FAIRCHILD, I.J., SPIRO, B., HERRINGTON, P.M. & SONG, T. 2000. Controls on Sr and C isotope compositions
 451 of Neoproterozoic Sr-rich limestones of East Greenland and North China. *In*: Grotzinger, J. P. &
 452 James, N. P. (eds) *Carbonate Sedimentation and Diagenesis in the Evolving Precambrian World*.
 453 SEPM (Society for Sedimentary Geology), 297–313.

454 FEDO, C.M. 2003. Detrital Zircon Analysis of the Sedimentary Record. *Reviews in Mineralogy and*
 455 *Geochemistry*, **53**, 277–303, doi: 10.2113/0530277.

456 GALBRAITH, R.F. 2005. *Statistics for Fission Track Analysis*. London, CRC Press.

457 HAN, Y., ZHAO, G., ET AL. 2016. Tarim and North China cratons linked to northern Gondwana through
 458 switching accretionary tectonics and collisional orogenesis. *Geology*, **44**, 95–98, doi:
 459 10.1130/G37399.1.

460 HOFFMAN, P.F. 1999. The break-up of Rodinia, birth of Gondwana, true polar wander and the
 461 snowball Earth. *Journal of African Earth Sciences*, **28**, 17–33, doi: 10.1016/S0899-
 462 5362(99)00018-4.

463 HOFMANN, M., LINNEMANN, U., RAI, V., BECKER, S., GÄRTNER, A. & SAGAWA, A. 2011. The India and South
 464 China cratons at the margin of Rodinia - Synchronous Neoproterozoic magmatism revealed by
 465 LA-ICP-MS zircon analyses. *Lithos*, **123**, 176–187, doi: 10.1016/j.lithos.2011.01.012.

466 HONG, Z., YANG, Y. & LIU, X. 1990. Archaeocyathid fossils from the lower Cambrian Jianchang
 467 Formation of the southern Liaodong Peninsula. *Geological Review*, **36**, 558–565.

468 HONG, Z., HUANG, Z. & LIU, X. 1991. Geology of Upper Precambrian in southern Liaodong Peninsula.
 469 *In: Special Reports on Geology from the Ministry of Geology and Mineral Resources, People's*
 470 *Republic of China*. Beijing, Geological Publishing House.

471 HUGHES, N., MYROW, P., ET AL. 2010. Cambrian rocks and faunas of the Wachi La, Black Mountains,
 472 Bhutan. *Geological Magazine*, **148**, 351–379, doi: 10.1017/S0016756810000750.

473 KIM, H.S. & REE, J.-H. 2016. Comments on 'Detrital zircon geochronology and Nd isotope
 474 geochemistry of the basal succession of the Taebaeksan Basin, South Korea: Implications for

475 the Gondwana linkage of the Sino-Korean (North China) Block during the Neoproterozoic–early
 476 Cambrian’ by . *Palaeogeography, Palaeoclimatology, Palaeoecology*, **459**, 610–612, doi:
 477 10.1016/j.palaeo.2016.04.024.

478 LEE, Y. IL, CHOI, T., LIM, H.S. & ORIHASHI, Y. 2016. Detrital zircon geochronology and Nd isotope
 479 geochemistry of the basal succession of the Taebaeksan Basin, South Korea: Implications for
 480 the Gondwana linkage of the Sino-Korean (North China) block during the Neoproterozoic–early
 481 Cambrian. *Palaeogeography, Palaeoclimatology, Palaeoecology*, **441**, 770–786, doi:
 482 10.1016/j.palaeo.2015.10.025.

483 LI, J., QIAN, M. & JIANG, Y. 2013. Overlapping of the Lower Cambrian Houjiashan Formation over the
 484 Pre-Cryogenian sequences in the Northern Jiangsu and Anhui Provinces. *Journal of*
 485 *Stratigraphy*, **37**, 232–241.

486 LI, Z.-X., EVANS, D.A.D. & HALVERSON, G.P. 2013. Neoproterozoic glaciations in a revised global
 487 palaeogeography from the breakup of Rodinia to the assembly of Gondwanaland. *Sedimentary*
 488 *Geology*, **294**, 219–232, doi: 10.1016/j.sedgeo.2013.05.016.

489 LIN, J.-L., FULLER, M. & ZHANG, W.-Y. 1985. Paleogeography of the North and South China Blocks
 490 during the Cambrian. *journal of geodynamic*, **2**, 91–114.

491 LIU, Y. 2012. *Restudy on Jianchang Formation and Trilobite Fauna of the Early Cambrian in Eastern*
 492 *Liaoning*. Shenyang Normal University.

493 LUO, C., ZHU, M. & REITNER, J. 2016. The Jinxian Biota revisited: taphonomy and body plan of the
 494 Neoproterozoic discoid fossils from the southern Liaodong Peninsula, North China.
 495 *Paläontologische Zeitschrift*, doi: 10.1007/s12542-016-0289-5.

496 MCKENZIE, N.R., HUGHES, N.C., MYROW, P.M., XIAO, S. & SHARMA, M. 2011a. Correlation of
 497 Precambrian–Cambrian sedimentary successions across northern India and the utility of
 498 isotopic signatures of Himalayan lithotectonic zones. *Earth and Planetary Science Letters*, **312**,
 499 471–483, doi: 10.1016/j.epsl.2011.10.027.

500 MCKENZIE, N.R., HUGHES, N.C., MYROW, P.M., CHOI, D.K. & PARK, T. -Y. 2011b. Trilobites and zircons link
 501 north China with the eastern Himalaya during the Cambrian. *Geology*, **39**, 591–594, doi:
 502 10.1130/G31838.1.

503 MEERT, J.G. & LIEBERMAN, B.S. 2008. The Neoproterozoic assembly of Gondwana and its relationship
 504 to the Ediacaran–Cambrian radiation. *Gondwana Research*, **14**, 5–21, doi:
 505 10.1016/j.gr.2007.06.007.

506 MIAO, L. 2014. *Biostratigraphy of the Basal Cambrian Xinji Formation and the Houjiashan Formation*
 507 *from the Southern North China Plate*. University of Chinese Academy of Sciences.

508 MURPHY, M.A. & SALVADOR, A. 1999. International Stratigraphic Guide - An abridged version. *Episodes*,

509 **22**, 255–271.

510 MYROW, P.M., HUGHES, N.C., ET AL. 2010. Extraordinary transport and mixing of sediment across
511 Himalayan central Gondwana during the Cambrian-Ordovician. *Geological Society of America*
512 *Bulletin*, **122**, 1660–1670, doi: 10.1130/B30123.1.

513 MYROW, P.M., CHEN, J., ET AL. 2015. Depositional history, tectonics, and provenance of the Cambrian-
514 Ordovician boundary interval in the western margin of the North China block. *Geological*
515 *Society of America Bulletin*, **127**, 1174–1193, doi: 10.1130/B31228.1.

516 NATIONAL COMMISSION ON STRATIGRAPHY OF CHINA & CHINA GEOLOGICAL SURVEY. 2014. *The Stratigraphic*
517 *Chart of China (2014)*. Beijing, Geological Publishing House.

518 NEDIN, C., JENKINS, R.J.F. & MOUNT, J.F. 1991. Re-Evaluation of Unconformities Separating the
519 ‘Ediacaran’ and Cambrian Systems, South Australia. *PALAIOS*, **6**, 102, doi: 10.2307/3514959.

520 PEARCE, N.J.G., PERKINS, W.T., WESTGATE, J.A., GORTON, M.P., JACKSON, S.E., NEAL, C.R. & CHENERY, S.P.
521 1997. A Compilation of New and Published Major and Trace Element Data for NIST SRM 610
522 and NIST SRM 612 Glass Reference Materials. *Geostandards and Geoanalytical Research*, **21**,
523 115–144, doi: 10.1111/j.1751-908X.1997.tb00538.x.

524 PEI, F. & FENG, W. 2005. Discovery of the Molluscan fauna from the lower Cambrian Xinji Formation
525 of Zhuyang, Lingbao of Henan. *Journal of Stratigraphy*, 458–461.

526 PETERS, S.E. & GAINES, R.R. 2012. Formation of the ‘Great Unconformity’ as a trigger for the Cambrian
527 explosion. *Nature*, **484**, 363–366, doi: 10.1038/nature10969.

528 QIAN, M., YUAN, X., LI, J., YAN, Y. & WANG, P. 2001. Comments on the Cambrian–Neoproterozoic
529 boundary in Huaibei district, northern Anhui-Jiangsu. *Journal of Stratigraphy*, 135–143.

530 QIAN, M., YUAN, X., XU, X., HU, J. & LI, J. 2002. An Assemblage of the Neoproterozoic Stromatolites
531 from the Xuzhou-Huainan Region. *Acta Palaeontologica Sinica*, **41**, 403–418.

532 QIAO, X. 2002. Seismic event, sequence and tectonic significance in Canglangpu Stage in Paleo-Tanlu
533 Fault Zone. *Science in China Series D*, **45**, 781, doi: 10.1360/02yd9078.

534 RAO, D.C. V, SANTOSH, M. & KIM, S.W. 2012. Cryogenian volcanic arc in the NW Indian Shield: Zircon
535 SHRIMP U-Pb geochronology of felsic tuffs and implications for Gondwana assembly.
536 *Gondwana Research*, **22**, 36–53, doi: 10.1016/j.gr.2011.10.014.

537 ROGOV, V., MARUSIN, V., ET AL. 2012. The oldest evidence of bioturbation on Earth. *Geology*, **40**, 395–
538 398, doi: 10.1130/G32807.1.

539 ROONEY, A.D., STRAUSS, J. V., BRANDON, A.D. & MACDONALD, F.A. 2015. A Cryogenian chronology: Two
540 long-lasting synchronous Neoproterozoic glaciations. *Geology*, **43**, 459–462, doi:
541 10.1130/G36511.1.

542 SHIELDS-ZHOU, G.A., HILL, A.C. & MACGABHANN, B.A. 2012. The Cryogenian Period. *In*: Gradstein, F. M.,

543 Ogg, J. G., Schmitz, M. D. & Ogg, G. M. (eds) *The Geologic Time Scale 2012*. Elsevier Science
 544 Limited, 393–411.

545 SHIELDS-ZHOU, G.A., PORTER, S. & HALVERSON, G.P. 2016. A New Rock-Based Definition for the
 546 Cryogenian Period (Circa 720–635 Ma). *Episodes*, **39**, 3–8, doi:
 547 10.18814/epiugs/2016/v39i1/89231.

548 SLÁMA, J., KOŠLER, J., ET AL. 2008. Plešovice zircon — A new natural reference material for U–Pb and Hf
 549 isotopic microanalysis. *Chemical Geology*, **249**, 1–35, doi: 10.1016/j.chemgeo.2007.11.005.

550 SQUIRE, R.J., CAMPBELL, I.H., ALLEN, C.M. & WILSON, C.J.L. 2006. Did the Transgondwanan
 551 Supermountain trigger the explosive radiation of animals on Earth? *Earth and Planetary Science*
 552 *Letters*, **250**, 116–133, doi: 10.1016/j.epsl.2006.07.032.

553 TANG, Q., PANG, K., YUAN, X., WAN, B. & XIAO, S. 2015. Organic-walled microfossils from the Tonian
 554 Gouhou Formation, Huaibei region, North China Craton, and their biostratigraphic implications.
 555 *Precambrian Research*, **266**, 296–318, doi: 10.1016/j.precamres.2015.05.025.

556 TORSVIK, T.H. & COCKS, L.R.M. 2013. New global palaeogeographical reconstructions for the Early
 557 Palaeozoic and their generation Harper, D. A. T. & Servais, T. (eds). *Geological Society, London,*
 558 *Memoirs*, **38**, 5–24, doi: 10.1144/M38.2.

559 TURNER, C.C., MEERT, J.G., PANDIT, M.K. & KAMENOV, G.D. 2014. A detrital zircon U–Pb and Hf isotopic
 560 transect across the Son Valley sector of the Vindhyan Basin, India: Implications for basin
 561 evolution and paleogeography. *Gondwana Research*, **26**, 348–364, doi:
 562 10.1016/j.gr.2013.07.009.

563 VAN LENTE, B., ASHWAL, L.D., PANDIT, M.K., BOWRING, S.A. & TORSVIK, T.H. 2009. Neoproterozoic
 564 hydrothermally altered basaltic rocks from Rajasthan, northwest India: Implications for late
 565 Precambrian tectonic evolution of the Aravalli Craton. *Precambrian Research*, **170**, 202–222,
 566 doi: 10.1016/j.precamres.2009.01.007.

567 VERMEESCH, P. 2004. How many grains are needed for a provenance study? *Earth and Planetary*
 568 *Science Letters*, **224**, 441–451, doi: 10.1016/j.epsl.2004.05.037.

569 VERMEESCH, P. 2012. On the visualisation of detrital age distributions. *Chemical Geology*, **312–313**,
 570 190–194, doi: 10.1016/j.chemgeo.2012.04.021.

571 VERMEESCH, P., RESENTINI, A. & GARZANTI, E. 2016. An R package for statistical provenance analysis.
 572 *Sedimentary Geology*, **336**, 14–25, doi: 10.1016/j.sedgeo.2016.01.009.

573 WANG, G., ZHANG, S., LI, S., YAN, Y., DOU, S. & FANG, D. 1984. *Research on the Upper Precambrian of*
 574 *Northern Jiangsu and Anhui Provinces*. Hefei, Anhui Press of Science and Technology.

575 WANG, M. & YANG, Z. 1986. Discovery of the lower Cambrian Qiongzhusi Stage in southern Liaodong
 576 Peninsula. *Liaoning Geology*, **1**, 1–7.

577 WANG, Q., YANG, D. & XU, W. 2012. Neoproterozoic basic magmatism in the southeast margin of
578 North China Craton: Evidence from whole-rock geochemistry, U-Pb and Hf isotopic study of
579 zircons from diabase swarms in the Xuzhou-HuaiBei area of China. *Science China Earth*
580 *Sciences*, **55**, 1461–1479, doi: 10.1007/s11430-011-4237-7.

581 WILHEM, C., WINDLEY, B.F. & STAMPFLI, G.M. 2012. The Altaids of Central Asia: A tectonic and
582 evolutionary innovative review. *Earth-Science Reviews*, **113**, 303–341, doi:
583 10.1016/j.earscirev.2012.04.001.

584 XIAO, S., NARBONNE, G.M. & SHIELDS-ZHOU, G.A. 2012. The Ediacaran Period. In: Gradstein, F. M., Ogg,
585 J. G., Schmitz, M. D. & Ogg, G. M. (eds) *The Geologic Time Scale 2012*. Elsevier Science Limited,
586 413–435.

587 XIAO, S., SHEN, B., TANG, Q., KAUFMAN, A.J., YUAN, X., LI, J. & QIAN, M. 2014. Biostratigraphic and
588 chemostratigraphic constraints on the age of early Neoproterozoic carbonate successions in
589 North China. *Precambrian Research*, **246**, 208–225, doi: 10.1016/j.precamres.2014.03.004.

590 XING, Y. 1996. *Chinese Stratigraphy Catalog- Neoproterozoic*. Beijing, Geological Publishing House.

591 XUE, Y., CAO, R., TANG, T., YIN, L., YU, C. & YANG, J. 2001. The Sinian stratigraphic sequence of the
592 Yangtze region and correlation to the Late Precambrian strata of North China. *Journal of*
593 *Stratigraphy*, **25**, 207–234.

594 YANG, D.-B., XU, W.-L., XU, Y.-G., WANG, Q.-H., PEI, F.-P. & WANG, F. 2012. U–Pb ages and Hf isotope
595 data from detrital zircons in the Neoproterozoic sandstones of northern Jiangsu and southern
596 Liaoning Provinces, China: Implications for the Late Precambrian evolution of the southeastern
597 North China Craton. *Precambrian Research*, **216–219**, 162–176, doi:
598 <http://dx.doi.org/10.1016/j.precamres.2012.07.002>.

599 ZANG, W. & WALTER, M.R. 1992. Late Proterozoic and Early Cambrian microfossils and
600 biostratigraphy, northern Anhui and Jiangsu, central-eastern China. *Precambrian Research*, **57**,
601 243–323, doi: 10.1016/0301-9268(92)90004-8.

602 ZHAI, M., HU, B., ZHAO, T., PENG, P. & MENG, Q. 2015. Late Paleoproterozoic–Neoproterozoic multi-
603 rifting events in the North China Craton and their geological significance: A study advance and
604 review. *Tectonophysics*, **662**, 153–166, doi: 10.1016/j.tecto.2015.01.019.

605 ZHANG, S.-H., ZHAO, Y., YE, H. & HU, G.-H. 2016. Early Neoproterozoic emplacement of the diabase sill
606 swarms in the Liaodong Peninsula and pre-magmatic uplift of the southeastern North China
607 Craton. *Precambrian Research*, **272**, 203–225, doi: 10.1016/j.precamres.2015.11.005.

608 ZHANG, W. & ZHU, Z. 1979. Notes on some trilobites from the lower Cambrian Houjiashan Formation
609 in southern and southwestern parts of North China. *Acta Palaeontologica Sinica*, **18**, 513–526.

610 ZHAO, G. 2013. *Precambrian Evolution of the North China Craton*. Elsevier.

ZHAO, G., SUN, M., WILDE, S.A. & SANZHONG, L. 2005. Late Archean to Paleoproterozoic evolution of the North China Craton: key issues revisited. *Precambrian Research*, **136**, 177–202, doi: 10.1016/j.precamres.2004.10.002.

Figure captions

Fig. 1. (a) Overview map showing the eastern North China Craton and adjacent terrains, simplified from (Zhao et al. 2005). **(b)** Geological map of Huaibei region with sample localities. **(c)** Geological map of Dalian region with sample localities. Names of investigated sections are marked next to the sample localities.

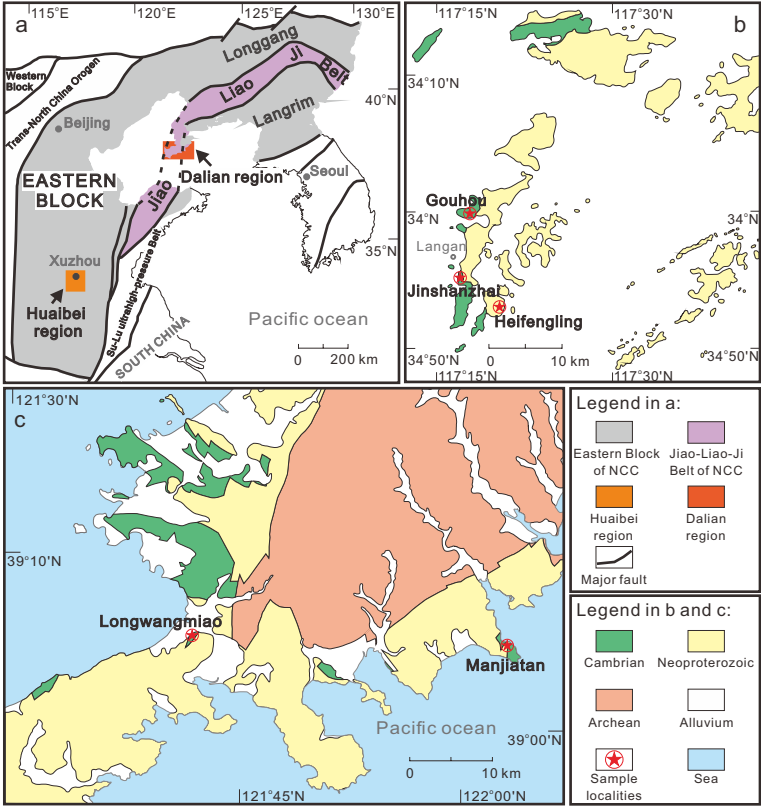


Fig. 2. Stratigraphic columns showing the investigated Tonian–Cambrian successions in Huaibei and Dalian regions. Columns are not to scale but thickness of individual formations at investigated sections is shown in bracketed under the formation name. Published fossil occurrences (Zhang & Zhu 1979, Hong et al. 1991, Zang & Walter 1992, Qian et al. 2002, Dong et al. 2008, Xiao et al. 2014, Tang et al. 2015, Luo et al. 2016), minimum depositional age constraints for Wangshan and Xingmuncun formations by U-Pb baddeleyite (By) or zircon (Zr) dating of cross-cutting diabase sills (Wang et al. 2012, Zhang et al. 2016), maximum depositional age (DZ) for Xingmuncun Formation using the youngest cluster of detrital zircon ages (Yang et al. 2012) are marked next to the stratigraphic column. Arrows point out the sampling horizons for detrital zircon dating in this study. Wave lines represent proposed unconformities.

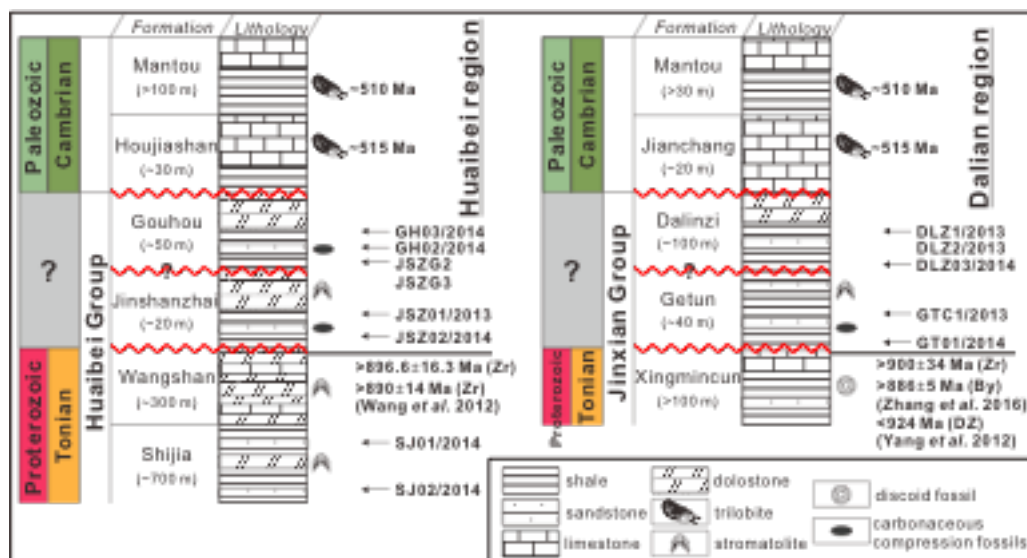


Fig. 3. Outcrop photos from Huaibei region: (a) unconformable contact between Wangshan and Jinshanzhai formations, Jinshanzhai section; (b) conglomerate bed exposed at the base of Jinshanzhai Formation, Jinshanzhai section; (c) unconformable contact between Gouhou and Jinshanzhai formations, Jinshanzhai section; (d) conglomerate bed exposed at the base of Gouhou Formation, Jinshanzhai section; clasts of stromatolite fragments possibly sourced from underlying Jinshanzhai Formation are marked by white circles; (e) red clastic rocks in the lower part of Gouhou Formation and carbonate in the upper part, Gouhou section; (f) halite pseudomorphs in the lower part of Gouhou Formation, Gouhou section; (g) Mottled (bioturbated) dolostone beds in the upper part of Gouhou Formation, Gouhou section; (h) Burrows in the upper part of Gouhou Formation, Gouhou section. Yellow lines illustrate the formation or member boundaries. Photo credits: YZ, TH, GS, LM, MZ and Martin Brasier.

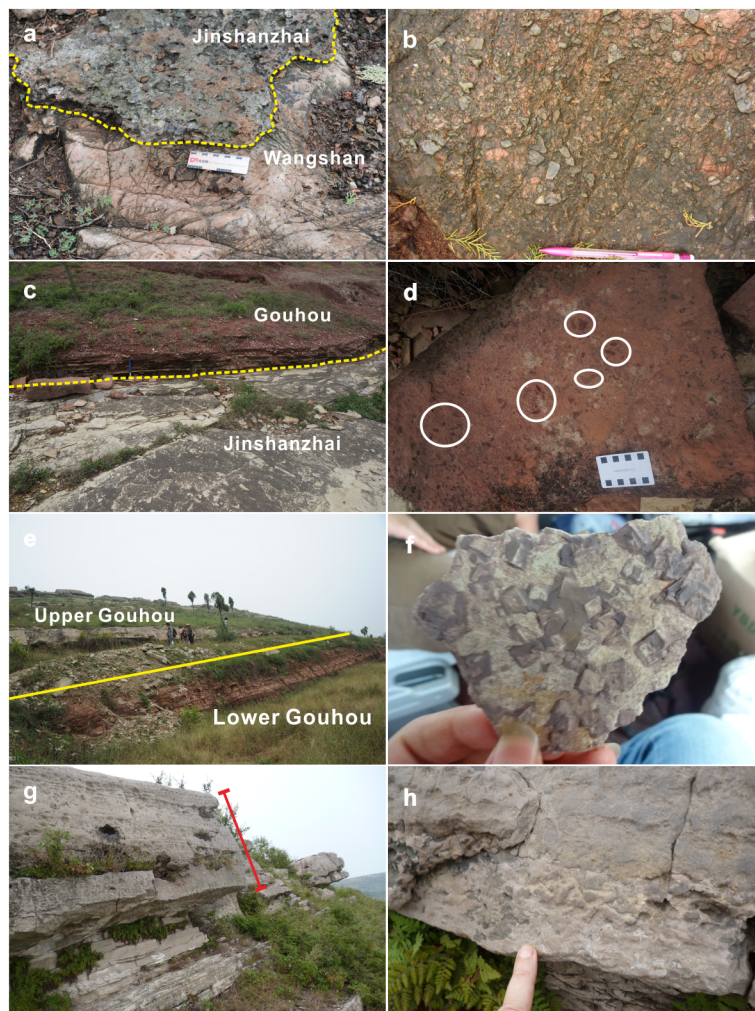


Fig. 4. Outcrop photos from Dalian region: (a) Disconformity between Xingmuncun and Getun formations, Manjiatan section; (b) exposure cracks in the topmost bed of the Xingmuncun Formation, Manjiatan section; (c) erosional surface between lower and middle parts of Getun Formation, Manjiatan section; (d) apparently transitional contact between Getun and Dalinzi formations, Manjiatan section; (e) black chert clasts near the contact between Getun and Dalinzi formations, Manjiatan section; (f) yellowish green and reddish purple sandstone of the Dalinzi Formation, Manjiatan section; (g) halite pseudomorphs marked by white circles in the Dalinzi Formation, Manjiatan section; (h) unconformable contact between Jianchang and Dalinzi formations, Manjiatan section; Yellow lines illustrate the formation or member boundaries. Photo credits: GS, TH, MZ.

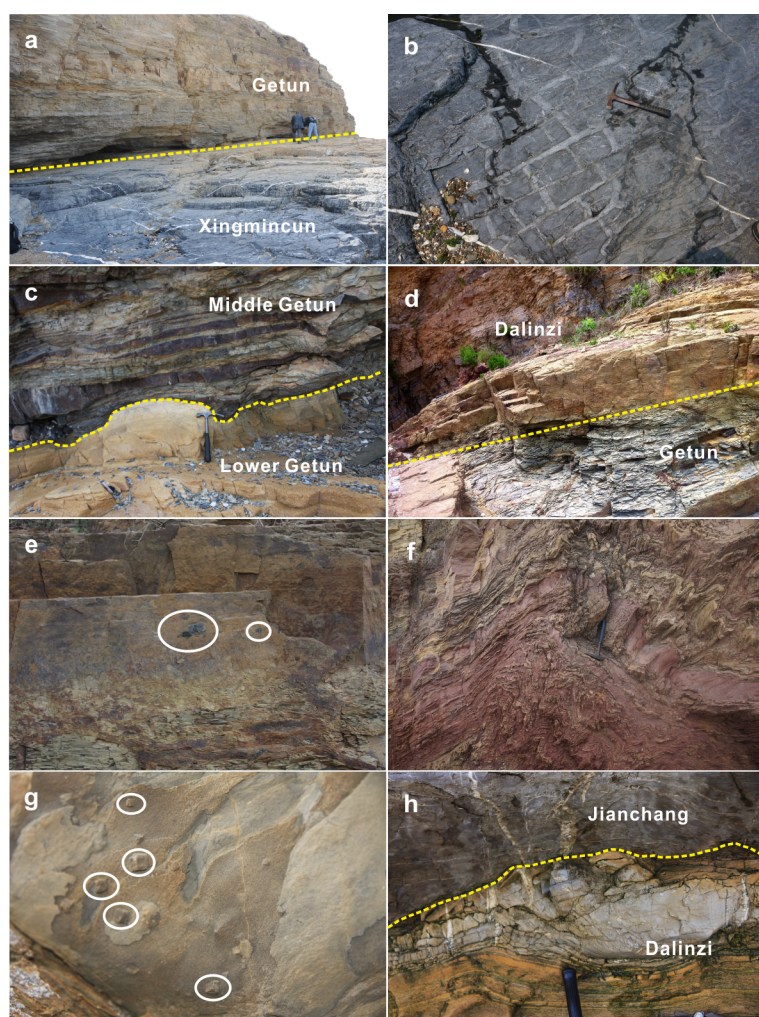


Fig. 5. Normalized kernel density estimate plots showing detrital zircon U-Pb ages from Tonian– Cambrian successions in southeastern North China Craton and eastern Korea. Maximum depositional ages of individual formations are illustrated. n: total number of zircon grains analysed. N: numbers of samples analysed.

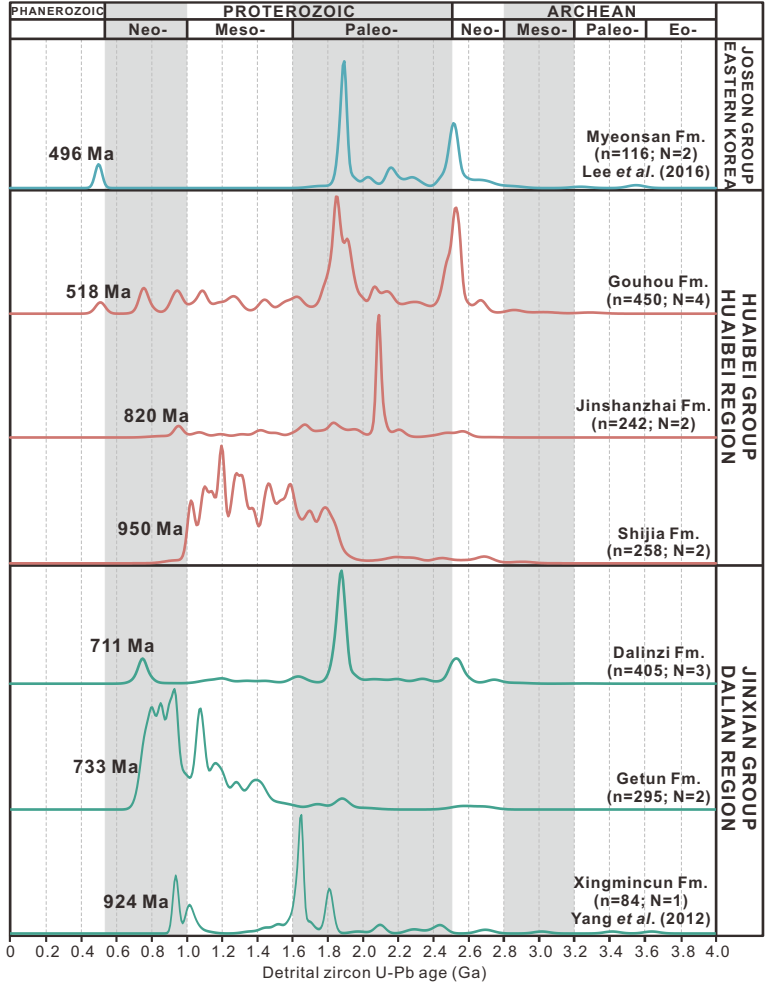


Fig. 6. Simplified chronostratigraphy with stratigraphic formations of the Neoproterozoic–Cambrian successions in southeastern North China Craton and eastern Korea, showing the regional unconformities at the Neoproterozoic–Cambrian transition. Red wave lines illustrate the unconformable contacts ('Great Unconformity') in contact with the major hiatus (grey area). Blue bands represent the intervals of major Cryogenian glaciations including Sturtian glaciation of ca. 717–662 Ma and Marinoan glaciation of ca. 645–635 Ma. (Rooney et al. 2015, Shields-Zhou et al. 2016) Question marks represent debatable unconformable contacts or undated boundaries. Ed. – Ediacaran; Cry. – Cryogenian;

